Structural Dynamics Research in a Full-Scale Transport Aircraft Crash Test

Harvey G. McComb Jr.,* Robert G. Thomson,† and Robert J. Hayduk‡
NASA Langley Research Center, Hampton, Virginia

A remotely piloted air-to-ground crash test of a full-scale transport aircraft was conducted for the first time for two purposes: 1) to demonstrate performance of an antimisting fuel additive in suppressing fire in a crash environment, and 2) to obtain structural dynamics data under crash conditions for comparison with analysis. The test, called the Controlled Impact Demonstration (CID), was sponsored by the Federal Aviation Administration (FAA) and the National Aeronautics and Space Administration (NASA) with cooperation of industry, the Department of Defense, and the British and French governments. The test aircraft impacted a Boeing 720 jet transport. The aircraft impacted a dry lake bed at Edwards Air Force Base. The FAA was interested in both the demonstration of performance of the antimisting fuel additive and the structural experiments. NASA's primary interest was structural dynamics research. Prior to the CID, drop tests were conducted on fuselage sections representative of the B 720 aircraft. These tests aided in the development of data acquisition equipment to measure crash response of the structure and mathematical models to calculate the structural crash behavior. The purpose of this paper is to discuss the structural aspects of the CID. The fuselage section tests and the CID itself are described. Structural response data from these tests are presented and discussed. Nonlinear analytical modeling efforts are described, and comparisons between analytical results and experimental results are presented.

Introduction

FOR over 35 years, full-scale crash tests have been conducted in the United States to help understand how aircraft structures behave in crash situations. Of particular interest are causes of passenger injury and fatalities resulting from severe, but potentially survivable, crashes. In the 1950s, the National Advisory Committee for Aeronautics conducted crash tests on light aircraft, fighters, and transports.[1,2] In the 1960s, the Federal Aviation Administration (FAA) conducted tests on a DC-7 and a Lockheed Constellation.[3,4] From 1972 to 1983, the National Aeronautics and Space Administration (NASA) conducted over 30 crash tests on general-aviation aircraft and helicopters.[5] All of these experiments were ground-based—either ground-to-ground runs into barriers or swing tests from a gantry into the ground. On December 1, 1984, the FAA and NASA conducted the first remotely piloted air-to-ground full-scale crash test of a transport aircraft. The aircraft, a Boeing 720 jet-powered transport, was remotely piloted to an impact point on the desert at Edwards Air Force Base, California. The test, called a full-scale transport controlled impact demonstration (CID), culminated four years of effort by the two agencies with the cooperation of industry, the Department of Defense, and the British and French governments.[6] The primary objectives of this experiment were: 1) to demonstrate a fuel additive called antimisting kerosene (AMK), intended to suppress crash-related fires, and 2) to gather crash dynamics data on airframe structure, seats, anthropomorphic dummies, and selected equipment. Organizational responsibilities for managing and executing this program are described in Refs. 6-8. The major responsibilities were carried by the FAA, NASA Ames Dryden Flight Research Center, and NASA Langley Research Center (LaRC).

The purpose of this paper is to describe the structural aspects of the CID and the fuselage section drop tests conducted before the CID. In addition, nonlinear analytical modeling efforts to predict both the fuselage section behavior in the station tests and the global airframe structural behavior in the CID are discussed.

Fuselage Section Tests

The goal of the research discussed in this paper was comparison of test and analysis results for the transport aircraft shown in Fig. 1. To help understand transport fuselage behavior under crash conditions, aid in development of mathematical models of the aircraft structure, and aid in development of data acquisition equipment, preliminary tests were conducted on fuselage sections. Three such tests were conducted at LaRC on 3.7-m (12-ft)-long sections of fuselage representing locations shown in Fig. 2. These fuselage test articles were actually from Boeing 707 aircraft, which have basically the same fuselage cross section as the Boeing 720.

The fuselage sections tested at LaRC were loaded with seats, anthropomorphic dummies, and instrumentation, but interior paneling, insulation, storage bins, and ducting had been removed. In each test, on the forward and center sections, nine anthropomorphic dummies were distributed among four or five triple seats.[9,10] Typically, ballast masses occupied remaining seat locations. In the aft fuselage section test, only one set of seats was installed. The remainder of the loading on that section consisted of equipment undergoing certification tests for the CID. The tests were performed in a vertical test apparatus, which provided a stable guide mechanism for the impact. In each test, the impact attitude was 0-deg pitch, yaw, and roll, and the impact velocity was 6.1 m/s (20 ft/s). The sections were dropped a little over 1.8 m (6 ft) and impacted on a concrete pad.

CID Test Aircraft

The aircraft used in this demonstration was a Boeing 720, four-engine, intermediate-range jet transport purchased new by the FAA in October 1960 (see Fig. 1). The aircraft was

Received Oct. 29, 1986; revision received Feb. 13, 1987.

*Distinguished Research Associate. Associate Fellow AIAA.
†Deceased; formerly Head, Impact Dynamics Branch.
‡Technical Assistant to Director for Structures. Member AIAA.

used for flight training of operations inspectors. Although the Boeing 720 is an old aircraft, its structural design and construction are still representative of narrow-body jet-transport aircraft currently in airline service.

Instrumentation layout of the aircraft is shown in Fig. 3. A total of 350 instruments were located throughout the aircraft, as listed in Table 1. The distribution was 45% on seats and dummies and 55% on structure. The vast majority of transducers (305) were accelerometers. The remaining 45 channels were strain-gage-type transducers. Seven major frames were instrumented from belly to crown with accelerometers (Fig. 3a). Cross-sectional views show the distribution of instrumentation at a particular frame. Eight strain-gage bending bridges were installed near these major frames. Wing instrumentation was limited, and primarily intended to measure vertical loads transmitted along the spars (Fig. 3b). Both inboard pylons had accelerometers at the engine connections to measure load transmission from engines to wings. For this project, LaRC developed and qualified all data acquisition equipment and a 10-camera onboard photographic system capable of withstanding the crash environment.

CID Impact Scenario

The impact scenario for the CID was selected after detailed study of 176 well-documented survivable jet-transport accidents that occurred between 1958 and 1979.[8,11] The planned scenario is illustrated in Fig. 4. The aircraft would follow a 3.3–4.0-deg glide slope in a 1-deg nose-up attitude with landing gear retracted. The aircraft would have a nominal sink rate of 5.2 m/s (17 ft/s) with no roll or yaw, a longitudinal velocity of 269–278 km/h (167–173 mph or 145–150 knots), and an aircraft gross mass of 79,400–88,500 kg (175,000–195,000 lbm). The planned impact, then, was to be symmetric for crash dynamics measurements followed by a slide through wing cutters and obstructions required for the AMK experiment. The intent was for the crash impact to be large enough to cause significant damage to the fuselage, but not so great as to cause complete fuselage breakup.

Mathematical Modeling

Mathematical models for structural analysis were developed for the fuselage section test articles and the complete B 720 CID test article using two computer programs—KRASH[12] and DYCAST.[13] KRASH was originally developed by Lockheed California Company and sponsored by the U.S. Army and the FAA. DYCAST was developed by Grumman Aerospace Corporation and sponsored by NASA and the FAA. DYCAST modeling is reviewed herein.

DYCAST

DYCAST is a nonlinear finite-element structural analysis computer program with dynamic capabilities. The basic element library consists of: 1) stringers, 2) nonlinear springs, 3) beams, 4) isotropic and orthotropic membranes, and 5) isotropic plates. The nonlinear spring element can be used as an elastic element, a dissipative element, or a gap element such as a ground-contact spring. The changing stiffness in

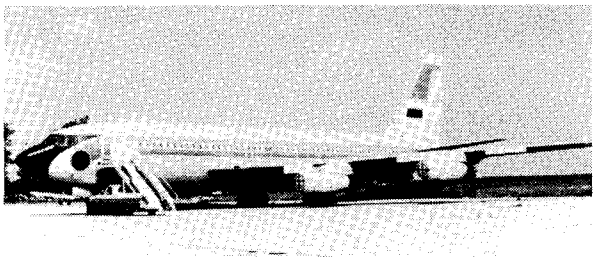

Fig. 1 Boeing 720 CID aircraft.

Table 1 CID instrumentation summary

Accelerometers	
Dummies	52
Seats	75
Structure	178
Overhead bins	3
Wing pylons	4
Wing other	14
Floor near seats	43
Frames	109
Center of gravity	3
Tail	3
Total	305
Bending bridges	
Wing	4
Fuselage	8
Total	12
Load cells	
Overhead storage bins	3
Lap belt	26
Shoulder harness	4
Total	33
Grand total—channels	350

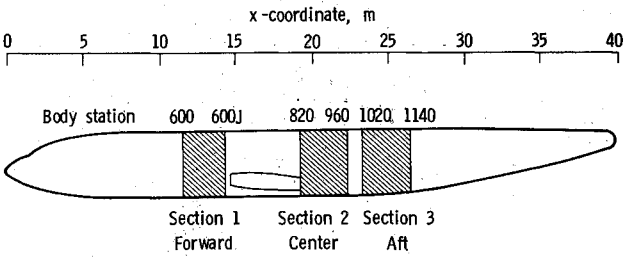

Fig. 2 Representative locations of fuselage drop test sections.

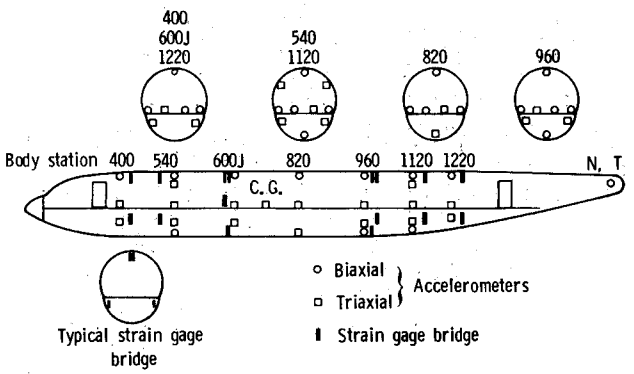

a) Fuselage.

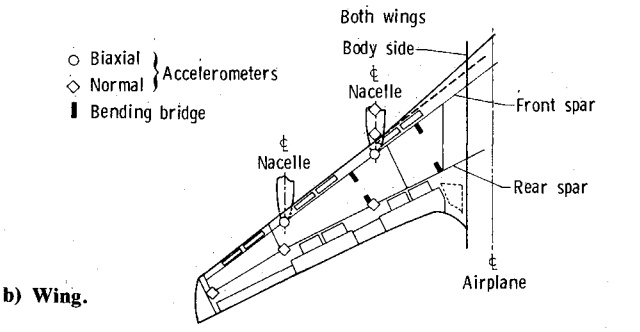

b) Wing.

Fig. 3 CID accelerometer and strain-gage locations.

the structure is accounted for by plasticity (material nonlinearity) and large displacements (geometric nonlinearity). Material nonlinearities are accommodated by one of three options: 1) elastic-perfectly-plastic, 2) elastic-linear-hardening-plastic, or 3) elastic-nonlinear-hardening-plastic of the Ramberg-Osgood type. Option 2 was used exclusively for this modeling effort. Geometric nonlinearities are handled in an updated Lagrangian formulation by reforming the structure into its deformed shape after small time increments while accumulating deformations, strains, and forces. The nonlinearities due to combined loadings (such as beam-column effects) are maintained, and stiffness changes due to structural failures are computed. The failure option is imposed automatically whenever a material failure strain criterion is met, or manually by the user at the restart of a simulation.

Numerical time integrators available are two explicit types—fixed-step central difference and modified Adams—and two implicit types—Newmark-beta and Wilson-theta. The latter three have a variable time-step capability, which is controlled internally by a solution convergence error measure. The Newmark-beta implicit time integrator was used exclusively for the calculations presented in this paper.

Descriptions of Models

Nonlinear dynamic calculations are very demanding of computer resources with current equipment. Therefore, careful attention must be focused on keeping the size and complexity of mathematical models under control. Boeing Commercial Airplane Company made major contributions to this modeling effort under contract to LaRC.

Fuselage Sections

Several different mathematical models were developed for fuselage sections with graduated degrees of refinement. Models of the forward section only are discussed here. Initially, a single frame model was developed, which included substantial detail of frame cross sections from crown to keel. Based on studies of this model, simplifications were identified that allowed reduction in the number of elements required to model a frame. Subsequently, the two-frame model shown in Fig. 5 was developed. This model contained sufficient detail to include the floor, two triple seats with lumped-mass occupants, and the basic fuselage structure without need for nonlinear springs to represent structure. Beam elements with appropriate cross-section shapes were used to model the frames below the floor, the floor itself, and seat rails. Less detail was used in modeling the upper fuselage.

The structure was assumed to be symmetric about the fuselage centerline, and computations were performed using a half-model. This half-model consisted of 105 degrees of freedom, 32 beams, 4 stringers, 16 lumped masses, 16 ground springs, and 4 seat springs. Nonlinear material properties for the subfloor frames (beam elements) were elastic-plastic with linear strain hardening. Detailed discussion of these models and results of fuselage section analyses are presented in Ref. 13.

CID Aircraft

A DYCAST model of the CID Boeing 720 aircraft was also developed. This model represents an aircraft 42 mm (137 ft) long and 40 m (131 ft) in wingspan. Detailed modeling for this complete aircraft in the mode used for the fuselage section models would require an excessive number of elements and degrees of freedom. Therefore, the CID model was developed using simple and compound beam elements along with nonlinear springs. A schematic sketch of the model is shown in Fig. 6.

The fuselage is modeled with a compound beam representing the cross-sectional properties of the skin-stringer-frame structure of the fuselage. The compound beam is formed by

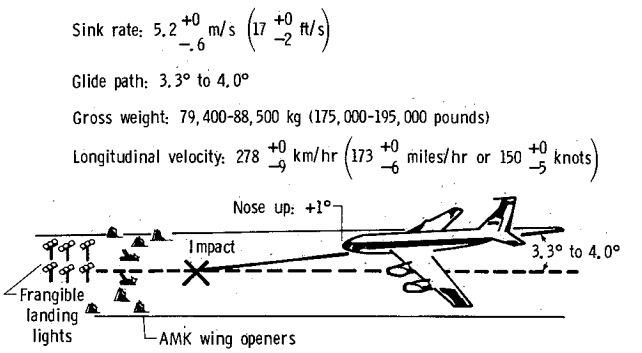

Fig. 4 Planned CID impact scenario.

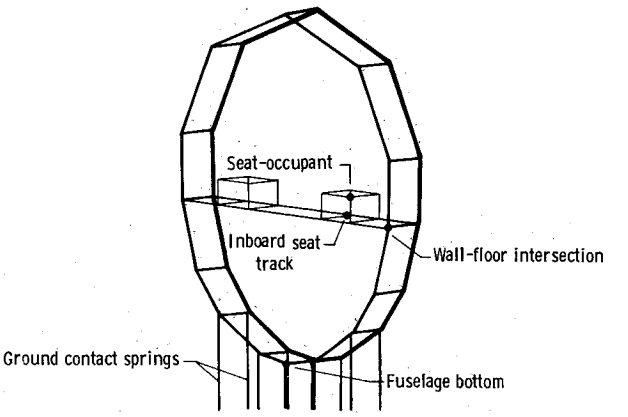

Fig. 5 Two-frame DYCAST mathematical model of fuselage section.

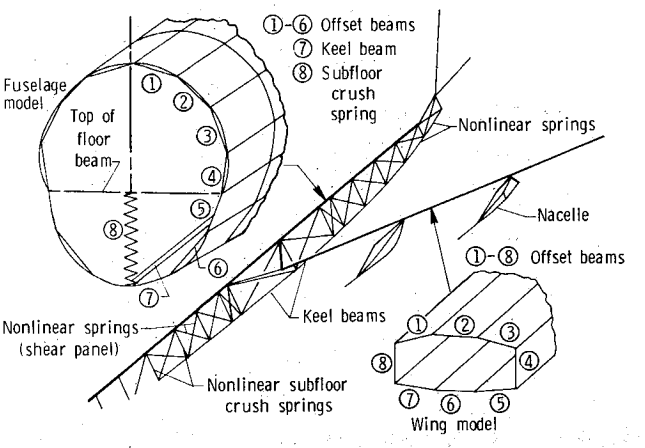

Fig. 6 DYCAST symmetric half-model of CID aircraft.

the combination of various beams representing cross-sectional segments of the fuselage constrained to bend as a unit. The elements shown in Fig. 6 underneath the compound beam representing the fuselage are nonlinear springs. They simulate fuselage crushing, and their properties are estimated from analyses of fuselage sections and results from fuselage drop tests.

Primary wing structure was modeled as a compound box beam. Engine and pylon structures were modeled as combinations of simple beams. In addition to the modeling indicated in the schematic drawings in Fig. 6, ground springs were included to represent the behavior of the impacted surface.

The planned impact scenario was to be symmetric ground impact—zero roll and zero yaw. Only one-half of the aircraft

was modeled, therefore. This model of half the aircraft consisted of 196 degrees of freedom, 126 beams (simple and compound), 113 concentrated masses, 73 structural crush springs, and 15 ground springs. External forces applied to the model were gravity, friction (using coefficient of friction of 0.4), and time-dependent lift.

Data Filtering

Both experimental and analytical results include a large high-frequency content that can mask the basic crash pulse information being sought. These high frequencies can be attributed to structural vibrations, which do not cause structural damage or trauma in occupants. Selection of proper filters to identify crash pulses that can potentially damage structure and cause trauma in occupants was the subject of extensive trials during the early part of the general-aviation aircraft crash dynamics research conducted at LaRC from 1972 to 1983. Based on this experience, all data presented in this paper (both experimental and analytical) were appropriately filtered as discussed in Ref. 14. For example, for dummy pelvis locations, a 180-Hz low-pass filter was used; for structural locations, a 100-Hz low-pass filter was used.

Results and Discussion

Fuselage Sections

Drop Tests

Results from drop tests of the forward and center fuselage sections are published in Refs. 9 and 10. Results from the drop test of the aft fuselage section are not yet published. A photograph of the forward fuselage drop test article after test is shown in Fig. 7. Gross structural damage was primarily confined to the lower fuselage. All seven frames of the fuselage section ruptured near the bottom contact point. Plastic hinges formed in each frame along both sides of the fuselage. The total posttest crushing distance varied from 0.56 to 0.58 m (22–23 in.) at the forward end (body station 600) to 0.46 to 0.48 m (18–19 in.) at the aft end (body station 600J). Motion-picture analysis of the forward frame at body station 600 indicated that a maximum deflection of approximately 0.66 m (26 in.) occurred 0.21 s after impact.

The behavior of the aft fuselage section in the drop test was similar to that of the forward section. Again, gross structural damage was confined to the lower fuselage, and frame rupturing and plastic hinging actions were similar to the forward section results. Maximum vertical pelvic accelerations in the dummies for both the forward and aft section tests were in the 6–8-*g* range (180-Hz filter).

The center section drop test results were startlingly different, however. The center section is an extremely stiff structure because it contains a sturdy keel structure that separates the main landing gear wheel wells. This center section deformed very little in the drop test. High dynamic loads were transmitted directly from the lower fuselage into the floor, upper fuselage, seats, and dummies. Limited failures occurred in the seat structure. Maximum vertical pelvis accelerations were in the 40–60-*g* (180-Hz filter), in contrast to results from the other two-section tests.

Comparisons Between Test and Analysis

Results are discussed from the forward fuselage section only. Values of 345 MPa (50 ksi) yield stress and 0.08 rupture strain were selected empirically to match roughly the overall experimental deformation behavior with the simple linear-strain-hardening plasticity option and the finite-element model used for these calculations. These values were used in all calculations for the fuselage section reported in this paper. Comparison between experimental and calculated vertical floor displacements as a function of time at body station 600 is shown in Fig. 8. Results for vertical accelerations as a function of time are shown in Fig. 9 at the joint between the fuselage wall and the floor at body station 600 (see Fig. 5). Results for vertical pelvis accelerations in an anthropomorphic dummy are shown in Fig. 10. Positive vertical acceleration is up. The experimental vertical acceleration histories show two distinct peaks. The first peak corresponds to the acceleration at initial contact. When the frames rupture at the bottom, load is relieved, and acceleration decreases. The second peak occurs at the time the frame plastic hinge points impact the concrete surface.

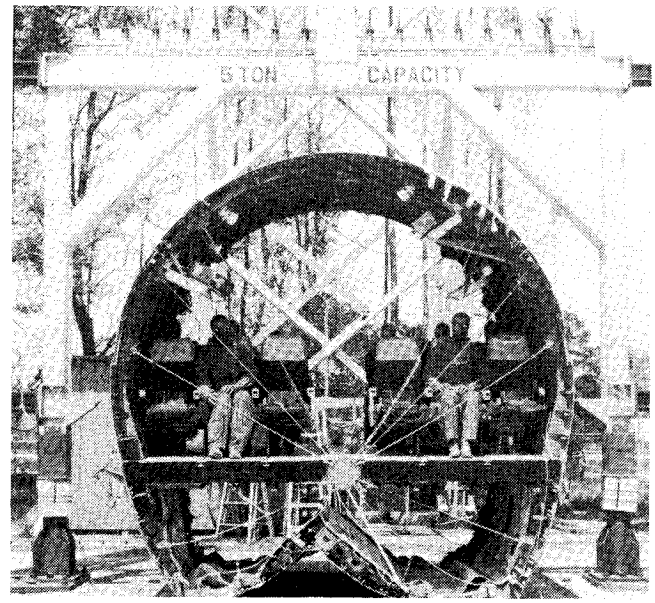

Fig. 7 Forward fuselage section after drop test.

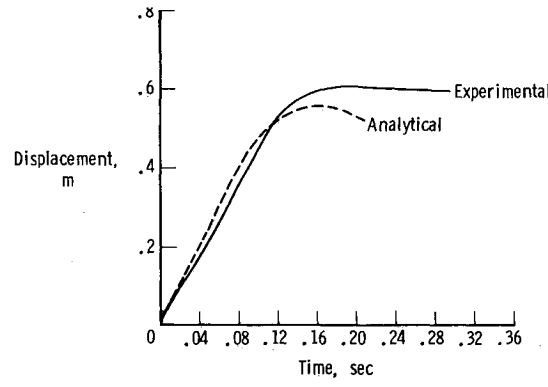

Fig. 8 Floor displacements in forward fuselage section drop test.

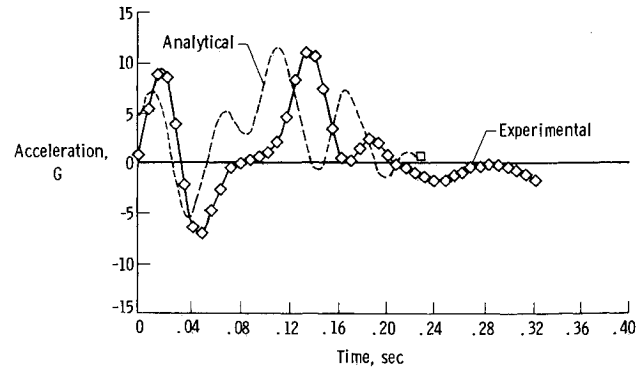

Fig. 9 Vertical accelerations at wall-floor interface in forward fuselage drop test.

The type of data presented in Fig. 8, for example, was used to model crush springs in the CID aircraft mathematical model. These comparisons in Figs. 8–10 do not display precise correlations between calculated and experimental results; however, the general trends are predicted, and maximum values of displacements and accelerations correlate reasonably well. Calculations for these plots were made with a constant time increment of 0.000250 s. Computer resources required for this model are indicated by the following data: to run 901 constant time increments (0.225 s real time) required 1620 s (central processing unit) on a Control Data Cyber 175 computer with a maximum field memory length of 303K.

CID Flight

Flight Test

At 9:13 a.m. Pacific Standard Time on Dec. 1, 1984, the CID aircraft took off from Edwards Air Force Base for its remotely piloted final flight. Weather conditions were ideal—visibility excellent and wind speed less than 5 knots. The aircraft was under ground-based control of an experienced NASA test pilot. The aircraft climbed to 700 m (2300 ft) above ground and circled the dry lake bed to intercept a simulated instrument landing system and begin its descent to the impact point. The instrument landing system and a video camera in the nose of the aircraft provided visual cues to aid the pilot.

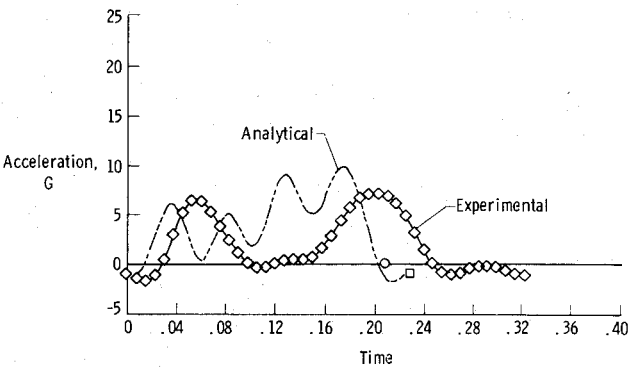

Fig. 10 Typical vertical pelvis accelerations in forward fuselage drop test.

At an altitude of 61 m (200 ft), the aircraft was off the target centerline, but not enough for the pilot to call a go-around. The 46-m (150-ft) altitude was the agreed-upon commit altitude because of activation of time-critical, limited-duration, onboard photographic and data acquisition equipment. At the 46-m (150-ft) altitude, the pilot made a left aileron control input to bring the aircraft back to the target centerline. The control input initiated lateral oscillations after commitment, but prior to impact. The pilot concentrated his efforts on damping the oscillations, achieving the best line-up possible with the target centerline, and meeting a critical project requirement of impacting the ground in front of the wing openers. The structural and seat experiments were planned for an impact and slideout prior to contacting the wing opener obstructions for the AMK experiment. Impacting beyond the wing openers would have jeopardized the AMK experiment if fuel spillage had not occurred.

Analysis of motion-picture film showed the actual CID crash scenario. A sequence of photographs illustrating the impact is presented in Fig. 11. The left outboard engine nacelle impacted the ground first at 9:22:11 a.m. The aircraft was rolled 13 deg to the left, yawed 13 deg to the left, and at zero pitch. The aircraft was traveling at a speed of 278 km/h (173 mph or 150 knots) with a sink rate of 5.27 m/s (17.3 ft/s) and an estimated gross mass of 87,090 kg (192,000 lbm). The initial impact occurred 125 m (410 ft) short of the planned impact point. After the left nacelles and wing impacted the ground, the aircraft continued to increase left yaw, and the fuselage pitched slightly nose down. Approximately 0.46 s after the initial impact and 86.9 m (285 ft) short of the planned impact point, the fuselage struck the ground at a pitch of −2.5 deg and a center-of-gravity sink rate of 3.66 m/s (12.0 ft/s). The wing, therefore, absorbed kinetic energy and reduced the severity of the fuselage impact. The aircraft yaw gradually increased to 38 deg left, and the first wing opener was contacted. This wing opener was third from the centerline among the four devices on the right-hand side of the aircraft. It cut through the right inboard nacelle and engine and diagonally slashed the leading edge and lower wing. The right wing failed, lifted upward as the aircraft continued to slide, and separated from the aircraft, dumping fuel during the process (Fig. 11). All four wing openers on the right side cut open the fuselage, which permitted fuel to enter the fuselage from the bottom. Because of the left yaw condition of the aircraft, none of the

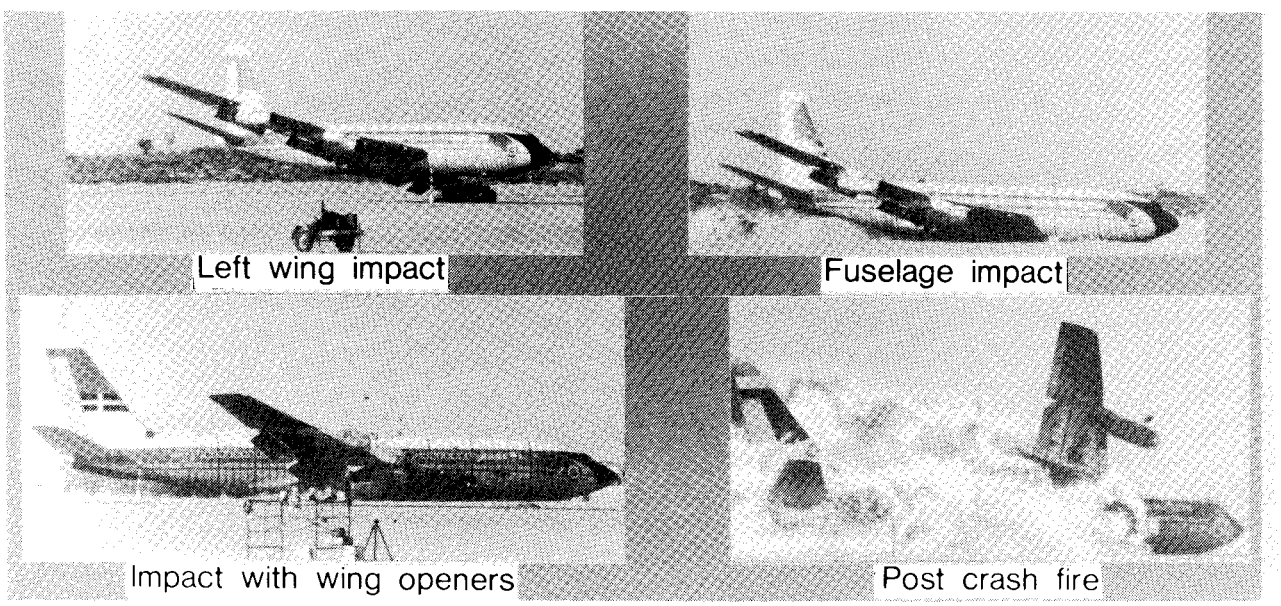

Fig. 11 CID impact sequence.

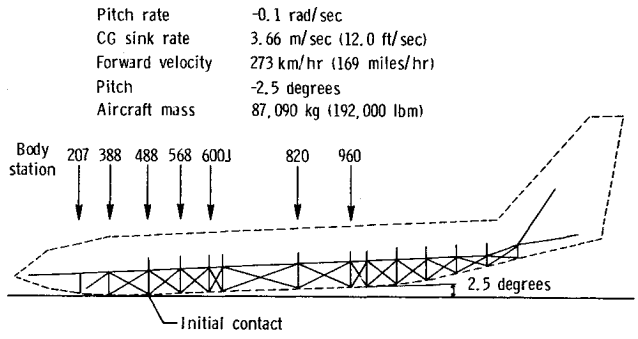

Fig. 12 DYCAST mathematical model at fuselage ground impact.

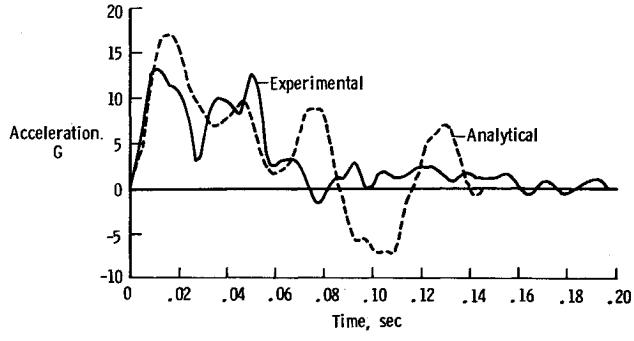

Fig. 13 Vertical floor accelerations at pilot location in CID.

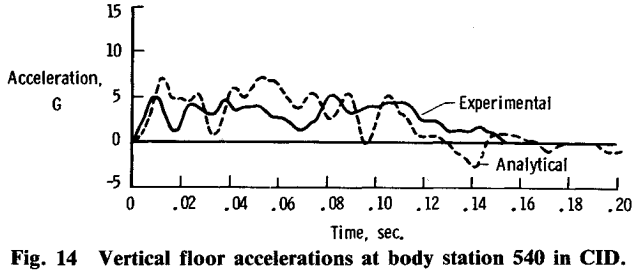

Fig. 14 Vertical floor accelerations at body station 540 in CID.

four wing openers on the left side of the aircraft struck the aircraft. At 9:22:21 a.m., the aircraft came to rest at a location about 290 m (950 ft) beyond the planned impact point. Results from the AMK experiment on the CID are in the publication process.[15,16]

Comparisons Between Test and Analysis

In April 1985, a workshop was held in Hampton, Virginia, to discuss all aspects of the crash dynamics experiments on the CID. Proceedings of that workshop containing a limited amount of structural dynamics data have been published in Ref. 14. Reference 17 presents a complete compilation of structural dynamics data in the form of acceleration and bending moment traces for 1 s after initial left wing impact and prior to wing cutter impact. Calculations were made with the symmetric DYCAST model discussed previously. Further calculations are currently in progress for a full airplane DYCAST model simulating the unsymmetric crash scenario that actually occurred, but results are not yet available.

Selected results from symmetric calculations are presented here and compared with corresponding test data from Ref. 17. Additional comparisons are contained in Ref. 13. The calculation began at the instant the fuselage contacted the

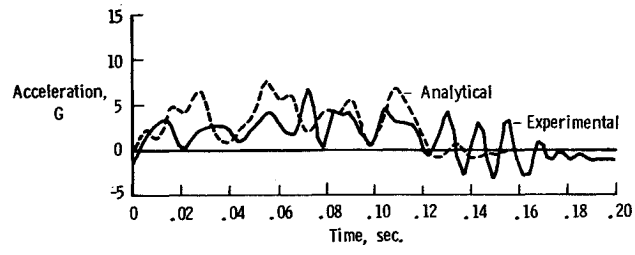

Fig. 15 Vertical floor accelerations at body station 600J in CID.

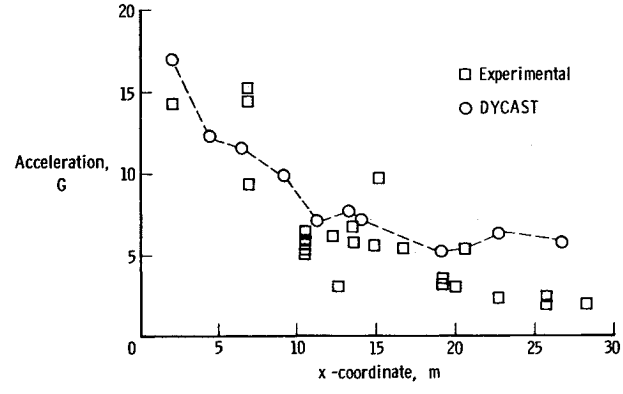

Fig. 16 Maximum vertical floor accelerations in CID.

ground and continued for 0.15 s. Initial conditions used in the analysis were established from the film coverage as follows: 75.7 m/s (248 ft/s or 147 knots) horizontal velocity and 3.66 m/s (12.0 ft/s) vertical velocity at the center of gravity, pitch of −2.5 deg, and pitch rate of −0.1 rad/s. A side view of the DYCAST model at time of initial fuselage contact is shown in Fig. 12. To introduce pitch rate into the model, the initial velocity of each finite-element joint was computed using the velocity vector of the center of gravity, the rotational velocity vector about the center of gravity, and the radius vector from the center of gravity to the joint. Yaw and roll conditions were ignored for this analysis.

Comparisons of experimental and analytical vertical floor accelerations are presented in Figs. 13–15 for three fuselage stations. Positive vertical acceleration is up. The solid lines are experimental data, and the dashed lines are analytical data. The general oscillatory behavior in the experimental data is predicted fairly well by the analysis, although the results are somewhat out of phase. The maximum values or peaks of the acceleration traces and the total 0.15-s crash pulse duration correlate reasonably well.

Comparisons of peak vertical floor accelerations are plotted as a function of distance along the fuselage in Fig. 16. Positive vertical acceleration is up. The square symbols are experimental data, and the circle symbols are analytical data. The analytical results display the same trends as the experimental results, and fairly well represent acceleration peaks for the length of the aircraft fuselage. Calculations for these plots were made with a constant time increment of 0.000500 s, which was conservative for this problem. Computer resources to run 300 constant time increments (0.150 s real time) required 1643 s (central processing unit) on a Control Data Cyber 175 computer with a maximum field memory length of 337K.

In Fig. 16, floor accelerations in the midfuselage region are reasonably in line with those in the fore and aft fuselage. The relatively high pelvic accelerations measured in the center section fuselage drop test (discussed in the section Results and Discussion, Fuselage Sections, Drop Tests) are

not reflected in the floor accelerations measured in the flight test of the complete airframe. Apparently, complete airframe response is more uniform than might be inferred from the fuselage section drop tests.

These comparisons between experimental and analytical accelerations are perhaps not as good as those for the fuselage sections. Nevertheless, the trends are fairly well predicted, and maximum values of accelerations correlate reasonably well. The mathematical models used in this work are not as refined as what is commonly used today to perform linear static stress analysis of transport aircraft structures. A building-block approach was used in which results from detailed models of structural components formed input to larger, but less detailed, models, leading finally to a full-airplane airframe model. The comparisons achieved with these analytical models and the experimental data indicate the validity of the basic strategy. It is felt, therefore, that the analytical approach typified in this paper can contribute substantially to understanding transport aircraft behavior under crash conditions.

Summary Remarks

A full-scale remotely piloted air-to-ground crash test was conducted on a Boeing 720 jet-transport aircraft, and drop tests were conducted on three fuselage sections representative of this aircraft. The large amount of structural dynamics data obtained is published elsewhere for use by engineers in the design of improved aircraft. Finite-element mathematical models were developed for structural analysis of these test articles, and experimental and analytical accelerations are compared. The mathematical models are not as refined as current state-of-the-art models for linear static stress analysis of transport aircraft and involve empirical input to represent crushing behavior of structure. Nevertheless, correlation among experimental and analytical accelerations is reasonably good. The analysis predicts trends and maximum values of local accelerations fairly well. These analyses are very demanding of current computer resources because of their dynamic nature. Future developments in analysis and computer technology will reduce the empiricism required for this type of calculation. It is believed, however, that the level of analysis reported here will continue to serve the engineering community to improve understanding of crash dynamics phenomena.

References

[1]Preston, G.M. and Pesman, G.J., "Accelerations in Transport-Airplane Crashes," NACA TN 4158, 1958.

[2]Acker, L.W., Black, D.O., and Moser, J.C., "Accelerations in Fighter Airplane Crashes," NACA RM E57G11, 1957.

[3]Reed, W.H., Robertson, S.H., Weinberg, L.W.T., and Tyndall, L.H., "Full-Scale Dynamic Crash Test of a Douglas DC-7 Aircraft," FAA-ADS-37, April 1965.

[4]Reed, W.H., Robertson, S.H., Weinberg, L.W.T., and Tyndall, L.H., "Full-Scale Dynamic Crash Test of a Lockheed Constellation Model 1649 Aircraft," FAA-ADS-38, Oct. 1965.

[5]Thomson, R.G., Carden, H.D., and Hayduk, R.J., "Survey of NASA Research on Crash Dynamics," NASA TP 2298, April 1984.

[6]Blake, N.A., "Controlled Impact Demonstration Review," SAE TP 851884, Oct. 1985.

[7]"Full-Scale Transport Controlled Impact Demonstration Program Management Plan," DOT/FAA/CT-82/151, Jan. 1984.

[8]Hayduk, R.J., Alfaro-Bou, E., and Fasanella, E.L., "NASA Experiments Onboard the Controlled Impact Demonstration," SAE TP 851885, Oct. 1985.

[9]Williams, M.S. and Hayduk, R.J., "Vertical Drop Test of a Transport Fuselage Section Located Forward of the Wing," NASA TM 85679, Aug. 1983.

[10]Williams, M.S. and Hayduk, R.J., "Vertical Drop Test of a Transport Fuselage Center Section Including the Wheel Wells," NASA TM 85706, Oct. 1983.

[11]Thomson, R.G. and Caiafa, C., "Structural Response of Transport Airplanes in Crash Situations," NASA TM 85654, June 1983.

[12]Soltis, S., Caiafa, C., and Wittlin, G., "FAA Structural Crash Dynamics Program Update—Transport Category Aircraft," SAE TP 851887, Oct. 1985.

[13]Fasanella, E.L., Widmayer, E., and Robinson, M.P., "Structural Analysis of the Controlled Impact Demonstration of a Jet Transport Airplane," *Journal of Aircraft*, Vol. 24, April 1987, pp. 274–280.

[14]Hayduk, R.J., compiler, "Full-Scale Transport Controlled Impact Demonstration," NASA CP 2395, 1986.

[15]Fenton, B.C., "Antimisting Fuel Technology Application in Full-Scale Transport Aircraft," DOT/FAA/CT-TN85/65, to be published.

[16]Yaffee, M.L., "Antimisting Fuel Research and Development for Commercial Aircraft," DOT/FAA/CT-86-7, to be published.

[17]Fasanella, E.L., Alfaro-Bou, E., and Hayduk, R.J., "Impact Data from the Controlled Impact Demonstration of a Transport Aircraft," NASA TP 2589, 1986.